



**HAL**  
open science

## **Expression patterns of RelA and c-mip are associated with different glomerular diseases following anti-VEGF therapy.**

Hassan Izzedine, Melanie Mangier, Virginie Ory, Shao-Yu Zhang, Kelhia Sendeyo, Vincent Audard, Christine Péchoux, Jean C. Soria, Christophe Massard, Rastilav Bahleda, et al.

### ► To cite this version:

Hassan Izzedine, Melanie Mangier, Virginie Ory, Shao-Yu Zhang, Kelhia Sendeyo, et al.. Expression patterns of RelA and c-mip are associated with different glomerular diseases following anti-VEGF therapy.. *Kidney International*, 2014, 85 (2), pp.457-70. 10.1038/ki.2013.344 . inserm-00958760

**HAL Id: inserm-00958760**

**<https://inserm.hal.science/inserm-00958760v1>**

Submitted on 28 Mar 2014

**HAL** is a multi-disciplinary open access archive for the deposit and dissemination of scientific research documents, whether they are published or not. The documents may come from teaching and research institutions in France or abroad, or from public or private research centers.

L'archive ouverte pluridisciplinaire **HAL**, est destinée au dépôt et à la diffusion de documents scientifiques de niveau recherche, publiés ou non, émanant des établissements d'enseignement et de recherche français ou étrangers, des laboratoires publics ou privés.



## C-mip and NF- $\kappa$ B define two distinct renal syndromes associated with VEGF-targeted therapy

Journal:	<i>Kidney International</i>
Manuscript ID:	Draft
Manuscript Type:	Basic Research
Date Submitted by the Author:	n/a
Complete List of Authors:	Izzedine, Hassane; Pitié-Salpêtrière Hospital, Nephrology; Mangier, Melanie; INSERM U955, Nephrology Ory, virginie; INSERM U955, Nephrology Zhang, Shao-yu; INSERM, UMR 955, Sendeyo, kélhia; INSERM U955, cell biology Audard, vincent; INSERM U955, Nephrology Pechoux, Christine; INRA, UR1196, plateforme MIMA2 Soria, Jean Charles; Institut Gustave Roussy, Medical Oncology Massard, Christophe; Institut Gustave Roussy, Medical Oncology Bahleda, Rastilav; Institut Gustave Roussy, Medical Oncology Bourry, Edward; Pitié-Salpêtrière Hospital, nephrology Khayat, David; Pitié-Salpêtrière Hospital, Medical Oncology baumelou, alain; Pitié-Salpêtrière Hospital, Nephrology Lang, philippe; INSERM, UMR 955, Ollero, Mario; INSERM, UMR 955, cell biology Pawlak, andre; INSERM, UMR 955, Sahali, Djilalli; INSERM, UMR 955,
Keywords:	clinical nephrology, transcription regulation, glomerular disease, glomerulopathy, Pathophysiology of Renal Disease and Progression
Subject Area:	Clinical Nephrology , Glomerular Disease, Renal Pathology

SCHOLARONE™  
Manuscripts

1  
2  
3 **C-mip and NF-kB define two distinct renal syndromes**  
4  
5 **associated with VEGF-targeted therapy**  
6  
7

8  
9 Hassan Izzedine<sup>1\*</sup>, Melanie Mangier<sup>2,3\*</sup>, Virginie Ory<sup>2,3</sup>, Shao-Yu Zhang<sup>2,3</sup>, Kelhia Sendeyo<sup>2,3</sup>,  
10 Vincent Audard<sup>2,3,7</sup>, C. Pécoux<sup>4</sup>, Jean Charles Soria<sup>5</sup>, Christophe Massard<sup>5</sup>, Rastilav  
11 Bahleda<sup>5</sup>, Edward Bourry<sup>1</sup>, David Khayat<sup>6</sup>, Alain Baumelou<sup>1</sup>, Philippe Lang<sup>2,3,7</sup>, Mario  
12 Ollero<sup>2,3</sup>, Andre Pawlak<sup>2,3</sup>, Djillali Sahali<sup>2,3,7</sup>.  
13  
14  
15  
16  
17

18  
19 Departments of <sup>1</sup>Nephrology, <sup>5,6</sup>Medical Oncology,

20  
21 <sup>1,5</sup>Pitié-Salpêtrière Hospital, Paris, France

22  
23 <sup>5</sup>Institut Gustave Roussy, Villejuif, France

24  
25 <sup>2</sup>INSERM, U 955, Equipe 21, F-94010, Créteil, France.

26  
27 <sup>3</sup>Université Paris-Est Créteil Val-de-Marne, F-94010, Créteil, France.

28  
29 <sup>4</sup>INRA, UR1196 Génomique et Physiologie de la Lactation, plateforme MIMA2, F-78352,  
30 Jouy-en-Josas Cedex, France  
31  
32

33  
34 <sup>7</sup>AP-HP, Groupe hospitalier Henri Mondor-Albert Chenevier, Service de Néphrologie, F-  
35 94010, Créteil, France.  
36  
37

38  
39 \* HI and MM contributed equally to this work

40 **Corresponding authors:**

41  
42 Hassane Izzedine and Djillali Sahali.

43  
44 Dr Hassane Izzedine, Service de Néphrologie, APHP, Université Pierre and Marie Curie,  
45 Paris VI, Groupe Hospitalier Pitié-Salpêtrière, Paris 75013, France.

46  
47 hassan.izzedine@psl.aphp.fr

48  
49 Dr Djillali Sahali, Service de Néphrologie, APHP, Université Paris-Est Créteil Val-de-Marne,  
50 UMRS 955, Equipe 21, Groupe hospitalier Henri Mondor-Albert Chenevier, Créteil, F-94010

51  
52 France. dil.sahali@inserm.fr  
53  
54  
55  
56  
57  
58  
59  
60

## Abstract

Renal toxicity constitutes a dose-limiting side effect of anticancer therapies targeting the vascular endothelial growth factor (VEGF). We studied twenty-nine patients having followed this kind of treatment. Eight of them developed minimal change nephropathy (MCN)/focal segmental glomerulopathy (FSG)-like lesions and thirteen thrombotic microangiopathy (TMA). MCN/FSG-like lesions developed mainly under receptor tyrosine kinase inhibitor (RTKI), whereas TMA complicated anti-VEGF therapy. Patients with TMA had no mutations in factors H, I, or membrane cofactor protein of the complement alternative pathway, while plasma ADAMTS13 activity persisted and anti-ADAMTS13 antibodies were undetectable. Glomerular VEGF expression was decreased in MCN/FSG and undetectable in TMA. Glomeruli of TMA displayed a high abundance of RelA in endothelial cells and in the podocytes nuclei, but *c-mip* was not detected. Conversely, MCN/FSG-like lesions exhibited a high abundance of *c-mip*, whereas RelA was scarcely detected. RelA binds in vivo to *c-mip* promoter and prevents its transcriptional activation, whereas knockdown of RelA releases the activation of *c-mip*. The RTKI sorafenib inhibits RelA activity and promotes *c-mip* expression. These observations suggest that *c-mip* and RelA define two distinct renal damages associated with VEGF-targeted therapies.

## Introduction

In renal glomeruli, podocytes express vascular endothelial growth factor (VEGF), whereas VEGF receptor tyrosine kinases are expressed by both podocytes and glomerular endothelial cells.<sup>1</sup> The biological functions of VEGF are mediated by its binding to one of the VEGF receptor tyrosine kinases (RTKs), which include VEGFR-1 (Flt-1), VEGFR-2 (KDR/Flk-1), and VEGFR-3 (Flt-4). The VEGF family comprises seven members, VEGF-A, -B, -C, -D, -E, and placenta growth factor 1 and 2 (PlGF1 and PlGF2). VEGF-A (also referred to as VEGF) binds to VEGFR-1 and -2, while VEGF-C and -D bind to VEGFR-2 and VEGFR-3. VEGFR2 expression has been reported in cultured podocytes.<sup>2</sup> Structurally, RTKs consist of an extracellular ligand-binding domain, a transmembrane region, and an intracellular, kinase domain that mediates downstream signal transduction. Upon binding to their ligand, RTKs dimerize and are phosphorylated on their kinase domain, leading to the recruitment of adaptor proteins that trigger intracellular signaling cascades important for processes such as cell proliferation and survival, migration and metabolism.<sup>3</sup> Dysregulation of RTK signaling by mutation or by ectopic receptor or ligand overproduction has been implicated in several aspects of tumor progression, including cell proliferation, survival, angiogenesis and tumor dissemination.<sup>4</sup>

VEGFR-2 is the predominant receptor in angiogenic signaling.<sup>5, 6</sup> VEGF is upregulated in response to hypoxia, oncogenes, or cytokines, and its expression is associated with poor prognosis in several types of cancer.<sup>7, 8</sup>

Experimental, preclinical and clinical studies have identified angiogenesis as a key process in the progression of most solid tumors. Thus, inhibition of VEGF and PDGF signaling is predicted to lead to anti-angiogenic effects and prevent the progression of tumors.<sup>9, 10</sup>

Therapeutic approaches targeting the VEGF ligand or RTK inhibitors (RTKIs) have recently

1  
2  
3 been developed. Several antagonists of VEGF signaling are being tested in clinical trials,  
4 including bevacizumab (anti-VEGF monoclonal antibody), and RTK inhibitors (RTKI) such  
5 as sunitinib, imatinib and sorafenib.<sup>11</sup> Although RTKI are widely used as inhibitors of  
6 VEGFRs, they interfere with the activity of other growth factors, among them PDGFRs, stem  
7 cell factor receptor (c-kit), FMS-like tyrosine kinase-3 (Flt-3), b-raf and Bcl-Abl. Thus, they  
8 are commonly named as multitargeted RTKI and widely used in medical oncology practice.  
9  
10 However, renal complications constitute a dose-limiting side effect of RTKI and anti-VEGF  
11 therapies.  
12

13  
14 We report here on a series of twenty-nine patients treated with anti-VEGF and RTKI who  
15 experienced proteinuria, hypertension and/or renal insufficiency. Immunomorphological and  
16 molecular studies suggest that RelA and c-mip define two separate glomerular damages  
17 associated with anti-angiogenic drugs.  
18  
19  
20  
21  
22  
23  
24  
25  
26  
27  
28  
29  
30  
31  
32  
33  
34  
35  
36  
37  
38  
39  
40  
41  
42  
43  
44  
45  
46  
47  
48  
49  
50  
51  
52  
53  
54  
55  
56  
57  
58  
59  
60

## Results

### *Clinical characteristics of patients with renal diseases*

Baseline patient characteristics are summarized in [Table 1](#). All patients were referred to a nephrology department because of discovery of proteinuria and/or increased serum creatinine following anti-VEGF initiating treatment. Sixteen patients had renal cell carcinoma and received 50 mg of sunitinib daily (n=11), 400 mg of sorafenib (n=3) or 5 mg axitinib (n=1) twice daily, or bevacizumab (10 mg/kg/dose) twice monthly (n=2). Thirteen other patients received VEGF Trap (4 to 6 mg/kg/dose) every three weeks (for ovarian, adrenal, breast, prostate, esophageal and rectal cancers), or bevacizumab 10 mg/kg/dose twice monthly (for lung, uterine and colorectal cancers). At the time of kidney biopsy, 20 patients (68,9%) presented with hypertension requiring antihypertensive treatment and 14 (48,3%) with renal failure defined by a creatinine clearance rate below 60 ml/min/1.73m<sup>2</sup>. Kidney biopsy was performed 2 to 12 weeks after the start of anti-VEGF treatment. Average number of glomeruli was 18.2 (range: 9-50). The principal pathological findings were TMA (n=13), MCN/FSG-like syndromes (n=8), acute tubular necrosis (n=3), and one case of each of the following lesions: membranous nephropathy, IgA nephropathy, ANCA negative pauciimmune crescentic glomerulonephritis, diabetic nephropathy and acute interstitial nephritis. Overlapping features of nephroangiosclerosis (7 patients) accompanied the other pathological findings. Fourteen patients (56%) died during the study due to cancer progression. Due to the expected limited survival, managing oncologists were reluctant to repeat the urinary investigations.

### *MCN/FSG like damages*

Eight patients with a previous nephrectomy for metastatic renal cell carcinoma (mRCC) and/or interferon alpha therapy exhibited MCN/FSG-like lesions, defined by nephrotic

1  
2  
3 proteinuria (with or without hypoalbuminemia), while light microscopy examination showed  
4  
5 either normal glomeruli or FSGS lesions. These patients had received sunitinib (5 patients),  
6  
7 sorafenib (2 patient) and Axitinib (1 patient). The mean interval between initiation of RTKI  
8  
9 therapy and onset of proteinuria was  $65 \pm 50.5$  days (range 14–180). All patients displayed  
10  
11 heavy proteinuria but only two exhibited hypertension and acute renal failure. Anti-VEGF  
12  
13 therapy was discontinued in all patients, and symptomatic treatments such as angiotensin  
14  
15 converting enzyme inhibitors or angiotensin-2 receptor antagonists were started. Six patients  
16  
17 died shortly thereafter due to cancer progression.  
18  
19

### 20 21 22 23 ***Renal thrombotic microangiopathy***

24  
25 Thirteen patients presented with renal TMA. Platinum derivatives (n=3), gemcitabine (n=1)  
26  
27 or radiotherapy (n=1) were administered prior to anti-VEGF agents. No clinical or biological  
28  
29 signs of TMA were observed during gemcitabine treatment, which was given six months  
30  
31 before the introduction of anti-VEGF medications. The mean interval between initiation of  
32  
33 anti-VEGF therapy and the onset of TMA was  $5.75 \pm 3.6$  months (range 2–12). Anti-VEGF  
34  
35 agents included bevacizumab (between 2 and 24 doses in six patients), VEGF Trap (after 2, 3,  
36  
37 4, 8, and 9 cycles in five patients, respectively) and sunitinib (after 2 cycles in two patients).  
38  
39 All patients showed significant proteinuria (including eight with nephrotic syndrome), while  
40  
41 eight had hypertension. Two patients developed acute renal failure and six displayed  
42  
43 microhematuria. Fifty percent of patients who developed TMA displayed haematological  
44  
45 manifestations. Anemia and thrombocytopenia were absent in 3 patients, while haptoglobin  
46  
47 was normal in 7 patients. Schistocytes were absent in 4 patients. Renal biopsies revealed  
48  
49 TMA in all patients, characterized by glomerular capillary thrombosis associated with  
50  
51 mesangiolytic and double contours. All patients exhibited normal complement proteins. No  
52  
53 constitutional abnormalities or heterozygous missense mutations were found in Factors H, I,  
54  
55  
56  
57  
58  
59  
60



1  
2  
3 or MCP, the 3 major regulatory proteins of the complement alternative pathway (CAP).  
4  
5 Plasma ADAMTS13 activity was above 20 percent. Acquired or constitutive anti-  
6  
7 ADAMTS13 antibodies were undetectable. Different symptomatic treatments were tried,  
8  
9 including plasmapheresis and fresh frozen plasma (7 patients), as well as steroid and  
10  
11 antihypertensive drugs. Renal and hematological symptoms were improved one to six months  
12  
13 after the discontinuation of anti-VEGF agents. Five patients died because to cancer  
14  
15 progression. One patient switched to another anti-VEGF agent (from VEGF Trap to  
16  
17 bevacizumab) and displayed an absence of proteinuria and stable renal function two years  
18  
19 later. Another patient continued bevacizumab in association with antihypertensive drugs for 8  
20  
21 months despite persistent proteinuria but renal function remained stable.  
22  
23  
24  
25  
26

27  
28 ***Differential expression of VEGF, HIF1 $\alpha$ , c-mip, RelA and Tie2 in glomeruli with TMA***  
29  
30 ***and MCN/FSG-like lesions***

31  
32 The relative abundance of VEGF was reduced in podocytes from patients with MCN/FSG  
33  
34 when compared to control kidney tissues and undetectable in TMA ([Figure 1a](#)), as previously  
35  
36 reported.<sup>12</sup>  
37

38  
39 Quantification of the relative abundance of c-mip, RelA, HIF1 $\alpha$  and Tie2, as well as their  
40  
41 expression pattern were analyzed in all glomeruli of MCN/FSGS or TMA biopsies and  
42  
43 compared to idiopathic forms (iMCNS, iFSGS and iTMA) ([Figure 1](#) and supplementary  
44  
45 Figure S1). For quantification, five biopsies corresponding to each pathological condition  
46  
47 were assessed and the data are depicted in [Figure 1f](#). The relative abundance of c-mip was  
48  
49 greatly increased in MCN/FSG-like lesions but no significant difference was observed with  
50  
51 idiopathic MCNS and FSGS diseases, whereas it was scarcely or not detected in TMA or in  
52  
53 control human kidneys ([Figure 1b and f](#)). Hypoxia-inducible factor 1 $\alpha$  (HIF-1 $\alpha$ ) is an  
54  
55 oxygen-sensitive transcription factor that is recruited in response to oxygen deprivation. We  
56  
57  
58  
59  
60

1  
2  
3 reasoned that in TMA ischemic conditions prevail and would result in a loss of oxygen  
4  
5 delivery to tissues, leading to HIF-1 $\alpha$  activation. In biopsies with MCN/FSG-like lesions,  
6  
7 HIF1 $\alpha$  expression was increased as compared with control human kidney, but higher  
8  
9 abundance was observed in TMA glomeruli without significant difference between  
10  
11 idiopathic- and VEGF forms ([Figure 1c and f](#)). Idiopathic MCNS and FSGS are considered  
12  
13 as non-inflammatory glomerular diseases.<sup>13</sup> We investigated whether, unlike the idiopathic  
14  
15 forms, inflammation may occur in MCN/FSG-like syndrome. Therefore, we analyzed the  
16  
17 expression of RelA, a master NF- $\kappa$ B transcription factor, which controls many inflammatory  
18  
19 genes.<sup>14</sup> The relative abundance of RelA was significantly higher in TMA than in control  
20  
21 human kidneys, whereas it was scarcely detected in MCN/FSG-like lesions ([Figure 1d and f](#)).  
22  
23 Subtle differences in RelA abundance and distribution were observed between anti-VEGF-  
24  
25 induced TMA and the idiopathic forms: RelA was uniformly increased in idiopathic TMA  
26  
27 glomeruli, but higher abundance was observed in anti-VEGF therapy-related TMA glomeruli  
28  
29 ([Figure 1f](#)) with a more restricted distribution to some capillary loops ([Figure 1d and](#)  
30  
31 [supplementary Figure S1](#)). On the other hand, RelA abundance was clearly reduced in  
32  
33 idiopathic MCNS and FSGS, as well as in MCN/FSG-like lesions, as compared with control  
34  
35 human kidneys, without significant difference between idiopathic forms and anti-VEGF-  
36  
37 related lesions ([Figure 1f](#)). The relative abundance of Tie2 was significantly increased after  
38  
39 anti-VEGF or RTKI therapies ([Figure 1e and f](#)).  
40  
41  
42  
43  
44  
45  
46  
47

48 Confocal microscopy analysis showed that nephrin expression was significantly reduced and  
49  
50 exhibited a granular pattern in MCN/FSG relatively to control human kidneys ([Figure 2](#)). In  
51  
52 contrast, nephrin displayed variable expression and an irregular pattern in TMA glomeruli  
53  
54 consisting of a lack of detection in some areas and preservation in others. In control human  
55  
56 kidneys, RelA was located on the external side of the specific endothelial cell marker Tie2  
57  
58  
59  
60

1  
2  
3 showing no colocalization, which suggests that RelA was only expressed in podocytes ([Figure](#)  
4  
5 [3](#)). The relative abundance of RelA was dramatically increased in TMA glomeruli, not only in  
6  
7 podocytes but also in endothelial cells, as shown by double labelling RelA/nephrin ([Figure 2](#))  
8  
9 and RelA/Tie2 ([Figure 3](#)), respectively. Tie2 immunostaining showed a slight increase in  
10  
11 MCN/FSG biopsies compared to control kidneys. Tie2 expression was strongly increased in  
12  
13 TMA with a diffuse, irregular pattern within the capillary loops ([Figure 3](#)). These results  
14  
15 suggest that in MCN/FSG-like syndromes associated with RTKI therapy, glomerular lesions  
16  
17 affect podocytes almost exclusively, whereas in TMA, alterations mainly affect endothelial  
18  
19 cells and podocyte injury may be a secondary event. Significant changes were also observed  
20  
21 in small arterioles in TMA biopsies, where endothelial cells were swollen and exhibited  
22  
23 higher abundance of RelA ([Figure 4](#)), when compared to endothelial cells from normal  
24  
25 arterioles. Moreover, arteriolar walls were infiltrated by pericytes that exhibited high amount  
26  
27 of RelA. These changes were not observed in the control human kidneys.

31  
32 We studied ultrastructural alterations in glomeruli of patients with bevacizumab-induced  
33  
34 TMA and in control kidneys (n=3 each). Transmission electron microscopy analysis showed  
35  
36 major alterations in TMA glomeruli including duplication of GBM, loss of fenestrations,  
37  
38 detachment of endothelial cells from original basement membrane, interposition of cells and  
39  
40 marked effacement of visceral epithelial cell foot processes in some areas. Some podocytes  
41  
42 exhibited cytoplasm vacuolization as well as endoplasmic reticulum enlargement and  
43  
44 mitochondrial swelling, suggesting an underlying apoptotic process ([Figure 5a](#)). To provide  
45  
46 accurate determination of RelA increase in bevacizumab-induced TMA, we performed  
47  
48 immunogold labeling and quantified the number of RelA gold particles in podocytes and in  
49  
50 endothelial glomerular cells. In TMA kidney biopsies, the number of RelA gold particles was  
51  
52 strongly increased in nuclear podocytes, as well as in endothelial glomerular cells as  
53  
54  
55  
56  
57  
58  
59  
60

1  
2  
3 compared with control kidney ( $p < 0.001$ ), while no significant difference was detected in the  
4  
5 cytoplasm of podocytes ([Figure 5b and c](#)).  
6  
7

### 9 **NF- $\kappa$ B binds to *c-mip* promoter and inhibits its transcriptional activity**

10  
11 Given the increased abundance of RelA in TMA contrasting with the virtual absence of *c-*  
12  
13 *mip*, we hypothesized that *c-mip* expression was repressed at the transcriptional level by NF-  
14  
15  $\kappa$ B. NF- $\kappa$ B-heterodimers bind to 10 bp  $\kappa$ B DNA sites that exhibit the consensus sequence (5'-  
16  
17 GGGRNWYYCC-3'), which comprises a constant core and a number of variable nucleotides  
18  
19 (R: A or G; N: any nucleotide; W: A or T; Y: C or T). The sequence identified on the human  
20  
21 *c-mip* promoter (*c-mip*- $\kappa$ B, 5'-GGGGCTGCCC-3') at position -199 to -214 (+1 corresponds  
22  
23 to the transcriptional initiation site) fulfils these criteria ([Figure 6a](#)). The mouse  $\kappa$ B response  
24  
25 element ( $\kappa$ B-RE) is identical to that of humans, except for the substitution of the T-nucleotide  
26  
27 by a C-nucleotide (5'-GGGGCCGCC-3'). To assess whether NF- $\kappa$ B binds to this sequence  
28  
29 *in vivo*, we performed chromatin immunoprecipitation using mouse podocytes. The short  
30  
31 region flanking the  $\kappa$ B-RE was precipitated by the anti-RelA antibody, but not by the rabbit  
32  
33 IgG control ([Figure 6b](#)). Incubation of nuclear extracts from HEK cells overexpressing RelA  
34  
35 with the radiolabeled *c-mip*  $\kappa$ B-RE oligonucleotide produced only one specific band shift in  
36  
37 EMSA ([Figure 6c](#)). The DNA binding shift appeared to be specific since it was abolished by  
38  
39 co-incubation with a mutated probe and shifted upwards in the presence of the anti-RelA  
40  
41 antibody. In contrast, the lower band shifts observed with the mutated *c-mip*- $\kappa$ B seemed to be  
42  
43 non-specific, as they were not altered by the preincubation of nuclear extracts with the anti-  
44  
45 RelA antibody. This result led us to study the effects of NF- $\kappa$ B on the transcriptional  
46  
47 activation of *c-mip*. The 877 bp full-length sequence containing the entire *c-mip* proximal  
48  
49 promoter was ligated upstream of the luciferase gene and cotransfected with NF- $\kappa$ B p50,  
50  
51 p65/RelA or both, as well as with the empty vector. Protein lysates were prepared 24 hours  
52  
53  
54  
55  
56  
57  
58  
59  
60

1  
2  
3 following transfection. Luciferase activity driven by the *c-mip* promoter was strongly reduced  
4  
5 in the presence of RelA ([Figure 6d](#)). Interestingly, overexpression of p50 alone did not inhibit  
6  
7 the transcriptional activity of *c-mip* promoter. Moreover, cotransfection of RelA with p50  
8  
9 significantly reduced the inhibition of luciferase activity induced by RelA alone. These results  
10  
11 suggest that RelA binds to the *c-mip* promoter and exerts a powerful inhibitory effect on *c-*  
12  
13 *mip* transcription. A strong argument supporting this hypothesis came from the study of wild-  
14  
15 type and RelA-deficient mouse embryonic fibroblasts (MEF). [Figure 7](#) shows that *c-mip* was  
16  
17 dramatically increased in RelA-deficient MEF, in the absence of any treatment, whereas it  
18  
19 was barely detected in wild-type MEF.  
20  
21  
22  
23  
24

#### 25 ***Sorafenib induces overexpression of c-mip in vivo and in vitro***

26  
27 We investigated whether overproduction of *c-mip* in MCN/FSG-like lesions is a secondary  
28  
29 molecular event or a direct effect of RTKI. At first, we tested whether sorafenib affects *c-mip*  
30  
31 expression in wild-type and RelA-deficient MEF. The abundance of *c-mip* is remarkably  
32  
33 higher in RelA-deficient MEF as compared with wild-type MEF ([Figure 8a](#)). However,  
34  
35 preincubation of cells with sorafenib increased the basal amount of *c-mip*, both in wild-type  
36  
37 and RelA-deficient MEF. We then treated a podocyte cell line with sorafenib and analyzed *c-*  
38  
39 *mip* expression by quantitative PCR. The abundance of transcript was significantly increased  
40  
41 in podocytes treated with sorafenib when compared with those incubated with the vehicle  
42  
43 only (ethanol) ([Figure 8b](#)). Because VEGF receptor is also expressed by lymphocytes, we  
44  
45 tested whether sorafenib affects *c-mip* expression in these immune cells. We purified  
46  
47 lymphocytes from normal donors by cell gradient density and incubated them with the same  
48  
49 concentration of sorafenib. Interestingly, *c-mip* was also increased in normal lymphocytes,  
50  
51 suggesting that the induction of *c-mip* by sorafenib was not restricted to podocytes ([Figure 8c](#)).  
52  
53  
54  
55  
56  
57  
58  
59  
60

### ***Sorafenib inhibits RelA activation***

In resting cells, RelA is mostly sequestered in the cytoplasm compartment by its inhibitor I $\kappa$ B $\alpha$ . Stimulation of cells by NF- $\kappa$ B inducers such as cytokines induces phosphorylation of I $\kappa$ B $\alpha$  at serine (Ser) residues 32-36, followed by its ubiquitination and proteasome degradation. RelA released from its inhibitor is phosphorylated and moves into the nucleus where it promotes transcriptional activation of target genes.<sup>15</sup> Phosphorylation of RelA at serine 276 plays a crucial role in NF- $\kappa$ B transcriptional activity.<sup>16</sup> Inhibition of RelA phosphorylation at serine 276 has been implicated in the transactivation inhibition of NF- $\kappa$ B–dependent genes.<sup>17</sup> Because RelA inhibits transcriptional activation of *c-mip*, we looked whether *c-mip* upregulation in MCN/FSG results from direct inhibition of RelA activity by RTKI therapy. Therefore, we treated the podocyte cell line with sorafenib and analyzed the activation status of RelA and its subcellular localization, as well as the stability of I $\kappa$ B $\alpha$ . In the absence of sorafenib, phospho-ser<sup>32-36</sup> I $\kappa$ B $\alpha$  was detected, along with phospho-ser<sup>276</sup> RelA, suggesting that NF- $\kappa$ B is constitutively activated in the podocytes ([Figure 9a](#)). Conversely, Sorafenib blocked RelA phosphorylation, whereas I $\kappa$ B $\alpha$  phosphorylation was significantly reduced, these effects were sustained for at least 48 hours. Immunoblotting of cytoplasm and nuclear podocyte extracts showed that Sorafenib induces accumulation of RelA in the cytoplasm, while very low abundance of RelA was detected in nuclear extracts ([Figure 9b](#)). In addition immunoprecipitation experiments showed that RelA was mostly sequestered with I $\kappa$ B $\alpha$  in podocytes incubated with Sorafenib ([Figure 9c](#)). Confocal microscopy analysis showed that RelA was diffusely expressed in both cytoplasm and nuclear compartment in untreated cells, whereas its expression was mostly restricted to cytoplasm in sorafenib-treated cells ([Figure 9d](#)). These results suggest that sorafenib inhibits NF- $\kappa$ B activity and indirectly promotes *c-mip* transcriptional activation.

1  
2  
3  
4  
5  
6  
7  
8  
9  
10  
11  
12  
13  
14  
15  
16  
17  
18  
19  
20  
21  
22  
23  
24  
25  
26  
27  
28  
29  
30  
31  
32  
33  
34  
35  
36  
37  
38  
39  
40  
41  
42  
43  
44  
45  
46  
47  
48  
49  
50  
51  
52  
53  
54  
55  
56  
57  
58  
59  
60

For Peer Review Only

## Discussion

Anti-VEGF therapy leads to various glomerular injuries, including MCN/FSG- and TMA-like syndromes. In our group of patients, we show for the first time that MCN/FSG lesions, which mostly observed following RTKI therapy, are associated with high abundance of *c-mip*. In contrast, in TMA resulting from anti-VEGF therapy, *c-mip* is not detected, while RelA is produced at high levels by podocytes and glomerular endothelial cells. We provide evidence that RelA binds to *c-mip* promoter *in vivo* and represses its transcription, while knock down of RelA releases this inhibition. These results may account for the non-expression of *c-mip* in the podocytes of patients with TMA. Conversely, inhibition of RelA activity promotes *c-mip* expression.

The association between occurrence of proteinuria and the inhibition of VEGF signaling is now established.<sup>18</sup> Despite the fact that our patients with MCN/FSG were older (mean, 71.5 yrs) as compared with TMA group (mean, 69.5 yrs) and had previously received interferon- $\alpha$ , proteinuria was negative before the introduction of RTKI therapy. Furthermore, patients did not receive any bisphosphonate, known to be toxic for podocytes. Finally, the development of proteinuria in all patients closely paralleled the administration of RTKI.

TMA has been reported to be associated with several anti-VEGF agents such as bevacizumab,<sup>19, 20</sup> VEGF Trap<sup>21</sup> and sunitinib,<sup>20, 22</sup> suggesting a class adverse effect. In our series, TMA was observed in 11/15 patients following bevacizumab and VEGF Trap therapies. These lesions were characterized by high abundance of RelA in endothelial cells and in podocytes.

The podocyte-specific deletion of VEGF in adult transgenic mice induces TMA.<sup>12</sup> In this model, thrombotic glomerular injury and heavy proteinuria precede the development of



1  
2  
3 hypertension, making hypertension unlikely to be the cause of proteinuria. In our patients  
4  
5 presenting with TMA, glomeruli exhibited high abundance of RelA, suggesting that abnormal  
6  
7 cell signaling induced by anti-VEGF treatment led to the recruitment of NF- $\kappa$ B and activation  
8  
9 of target genes at the sites of injury. Reduced endothelial NF- $\kappa$ B activity decreases  
10  
11 albuminuria independently of its effects on blood pressure in transgenic mice with endothelial  
12  
13 cell-restricted NF- $\kappa$ B super-repressor overexpression.<sup>23, 24</sup> The increase in intrarenal  
14  
15 angiotensin II induced by proteinuria depends on NF- $\kappa$ B activation. By inhibiting not only the  
16  
17 induction of proinflammatory cytokines but also the activation of the intrarenal renin-  
18  
19 angiotensin system, the inhibition of renal NF- $\kappa$ B activation may be therapeutically useful as  
20  
21 a means of retarding the development and progression of renal damage associated with  
22  
23 persistent proteinuria.<sup>25</sup> Our findings suggest that the inhibition of NF- $\kappa$ B could have a  
24  
25 beneficial effect in the management of TMA associated with anti-VEGF therapy.  
26  
27

28  
29 Several pathophysiological mechanisms have been put forward for the occurrence of  
30  
31 MCN/FSG-like lesions in patients undergoing RTKI therapy.<sup>18</sup> The high incidence of RCC in  
32  
33 our cohort (60%) suggests a possible role for the adaptive hyperfiltration response to  
34  
35 nephrectomy, as reported in the literature.<sup>26</sup> However, in our patients proteinuria was still  
36  
37 absent at least one year after nephrectomy and developed rapidly only after initiation of anti-  
38  
39 VEGF therapy, ruling out a potential close link between unilateral nephrectomy and  
40  
41 proteinuria, although we cannot exclude the possibility that the former may promote RTKI-  
42  
43 induced podocyte injury.  
44  
45

46  
47 Several signaling molecules have been shown to interact with VEGFR2 including the  
48  
49 regulatory p85 subunit of PI3-kinase,<sup>27</sup> Fyn and Nck.<sup>28</sup> VEGFR-2 is rapidly phosphorylated in  
50  
51 response to VEGF and leads to the recruitment of Fyn, which then initiates a cascade of  
52  
53 phosphorylation events involving Nck, PAK-2 and N-WASP, resulting in actin  
54  
55 polymerization and actin stress-fiber formation.<sup>28, 29</sup>  
56  
57  
58  
59  
60

1  
2  
3 VEGFR2 expression in podocytes is still debated. Compelling evidence suggests that  
4 VEGFR2 is expressed in a differentiated podocyte cell line,<sup>2</sup> as well as in mouse podocytes.<sup>30</sup>  
5  
6 Moreover, VEGFR2 interacts *in vitro* and *in vivo* with nephrin, a specific podocyte marker.<sup>31</sup>  
7  
8 Although these data suggest that podocytes possess a functional autocrine VEGF-VEGFR2  
9 system, another group has failed to detect VEGFR2 in podocytes *in vivo*.<sup>32</sup> In addition, this  
10 group has shown that knockdown of VEGFR2 in podocytes has no effect on glomerular  
11 development and function.  
12

13  
14 The data presented here strongly suggest that RelA is a repressor of c-mip. Because RelA is  
15 constitutively expressed in podocytes, the lack of c-mip detection in control glomeruli is not  
16 unexpected. Conversely, inhibition of NF-κB activity by RTKI therapy, also reported by other  
17 authors,<sup>33</sup> leads to c-mip overexpression and induces human podocyte disease with nephrotic  
18 proteinuria, reminiscent of the transgenic c-mip mouse model.  
19

20  
21 We have recently reported that c-mip abundance increases in the podocytes of patients with  
22 acquired idiopathic nephrotic syndromes, including primary MCNS and FSGS, in which  
23 podocytes are the main target of injury.<sup>34</sup> Transgenic mice that overexpress c-mip in  
24 podocytes develop heavy proteinuria without inflammatory lesions or cell infiltration. We  
25 have shown that c-mip turns off podocyte signaling by preventing the interaction of nephrin  
26 with Fyn, thereby decreasing nephrin phosphorylation *in vitro* and *in vivo*.<sup>34</sup> We have also  
27 shown that c-mip inhibits the interaction between Nck and nephrin and between Fyn and N-  
28 WASP, potentially accounting for cytoskeletal disorganization and the effacement of foot  
29 processes.<sup>34</sup> Moreover, the intravenous injection of a small interfering RNA (siRNA)  
30 targeting c-mip prevents lipopolysaccharide-induced proteinuria in mice.<sup>34</sup> These results  
31 suggest that c-mip plays a crucial role in podocyte dysfunction leading to proteinuria.  
32

33  
34 Renal TMA is a serious complication that usually leads to drug withdrawal.<sup>12, 19-22</sup> The  
35 physician must be aware of these rare complications, institute surveillance for renal  
36  
37  
38  
39  
40  
41  
42  
43  
44  
45  
46  
47  
48  
49  
50  
51  
52  
53  
54  
55  
56  
57  
58  
59  
60

dysfunction and thoroughly investigate patients who develop hematological or renal abnormalities while receiving therapy. Cessation of these agents is of particular clinical relevance, given the loss of their impressive therapeutic potential in a range of cancers.

For Peer Review Only

1  
2  
3  
4  
5  
6  
7  
8  
9  
10  
11  
12  
13  
14  
15  
16  
17  
18  
19  
20  
21  
22  
23  
24  
25  
26  
27  
28  
29  
30  
31  
32  
33  
34  
35  
36  
37  
38  
39  
40  
41  
42  
43  
44  
45  
46  
47  
48  
49  
50  
51  
52  
53  
54  
55  
56  
57  
58  
59  
60

## Material and Methods

### *Selection of patients*

Twenty-nine patients who developed a renal syndrome following VEGF-targeted therapy underwent kidney biopsy. The clinical and laboratory studies were assessed at the time of renal biopsy and follow-up data were available for all patients (Table 1). Each patient was followed over time for the development of specific end points, including progression to severe renal failure and death.

Controls include adult patients with idiopathic glomerular diseases (MCNS, FSGS and TMA). Control renal samples (n=5) were supplied by the hospital tissue bank (platform of biological resources, Henri Mondor hospital) from patients undergoing nephrectomy for polar kidney tumor and were considered as normal by the pathologists.

### *Complement assays and ADAMTS13 plasma activity*

Plasma concentrations of complement factor H (CFH) and factor I (CFI) were measured by enzyme-linked immunosorbent assay (ELISA), and serum levels of C4, C3, and factor B (FB), by nephelometry. Membrane cofactor protein (MCP or CD46) expression was analyzed in granulocytes using phycoerythrin (PE)-conjugated anti-CD46 antibodies (Serotec, Oxford, United Kingdom). Sequencing of CFH, CFI, and MCP genes, functional assays for ADAMTS13 plasma activity and tests for circulating antibodies to ADAMTS13 were performed as previously described.<sup>35, 36</sup>

### *Immunohistochemistry and confocal microscopy analyses*

Primary antibodies used in this study included anti-VEGF, anti-HIF-1 $\alpha$ , anti-Tie2, anti-NF- $\kappa$ B RelA and p50 (Santa Cruz Biotechnology, CA), anti-nephrin (Progen, Heidelberg, Germany) and anti-c-mip. Immunohistochemistry and immunofluorescence studies were

1  
2  
3 carried out in each group and specific labeling was quantified as previously described.<sup>34</sup> For  
4  
5 quantification, all glomeruli from each section, except those with significant sclerosis ( $\geq$   
6  
7 50%), were analyzed by computer-assisted image analysis using 400x magnification. The  
8  
9 images were blindly analyzed by two independent investigators, as previously described.<sup>37</sup>  
10  
11 Positive staining within each glomerulus was expressed as percentage of immunostained  
12  
13 area over total glomerular area using image analysis software (Image J; National Institute of  
14  
15 Health, Bethesda, USA).<sup>38</sup>  
16  
17  
18  
19

### 20 21 ***Transmission Electron microscopy and immunogold labeling***

22  
23 Tissues were fixed with 2% glutaraldehyde in 0.1 M Na cacodylate buffer pH 7.2, for 4 hours  
24  
25 at room temperature and then postfixed with 1% osmium tetroxide containing 1.5% potassium  
26  
27 cyanoferrate, contrasted with 2% aqueous uranyl acetate, gradually dehydrated in ethanol  
28  
29 (30% to 100%) and embedded in Epon (Delta microscopie, Labège France). Thin sections (70  
30  
31 nm) were collected onto 200 mesh cooper grids, and counter stained with lead citrate, then  
32  
33 examined under a Zeiss EM902 electron microscope. Electron micrographs were acquired  
34  
35 with a charge-coupled device camera MegaView III CCD camera and analysed with ITEM  
36  
37 software.  
38  
39

40  
41 For immunogold labeling, kidney biopsies (n=3) and controls (n=3) were successively fixed  
42  
43 with a mixture of 4% PFA/ 0.25% glutaraldehyde in 0.1 M phosphate buffer, pH 7.2 (PB) for  
44  
45 one hour, followed by 4% PFA, then processed for ultracryomicrotomy as described.<sup>39</sup> The  
46  
47 grids were placed on the 2% gelatine in a 37°C stove for 30 min, quenched with 50 mM  
48  
49 glycine in PB, blocked with 1% BSA and 10% normal goat serum (NGS), then incubated with  
50  
51 RelA antibody (1:30 dilution) in PB containing 1% BSA, 2% NGS for 2 hours. The grids  
52  
53 were washed twice, followed by incubation with goat anti-rabbit IgG coupled to 10 nm  
54  
55 colloidal gold particles (British Biocell International, UK). After washing, cryosections were  
56  
57  
58  
59  
60

1  
2  
3 stained with 2% uranyl acetate, and embedded with 2% methylcellulose containing 5% uranyl  
4  
5 acetate. Random capillary loops were scanned by transmission electron microscopy and the  
6  
7 number of gold particles in podocytes and in glomerular endothelial cells were counted and  
8  
9 expressed as the number of gold particles per square micrometer ( $\text{Au}/\mu\text{m}^2$ ).  
10

### 11 12 13 14 ***Cell culture with RTKI and reverse transcription-polymerase chain reaction (RT-PCR)***

15  
16 Conditionally immortalized mouse podocytes have been described elsewhere.<sup>40</sup> Sorafenib  
17  
18 (BAY 439006, Enzo Life Sciences Inc.) and Sunitinib malate (Sigma Aldrich) were  
19  
20 dissolved in ethanol and stored at minus 20°C before use. Differentiated podocytes were  
21  
22 exposed to 10 mM sorafenib for 30 hours at 37°C. Then, cells were washed three times in  
23  
24 PBS and total RNA was prepared using RNeasy kit (Qiagen, France). Reverse transcription  
25  
26 was performed with Superscript II (Invitrogen, Inc, CA) and PCR amplification with  
27  
28 Phusion high-fidelity DNA polymerase (Finnzyme, Finland). The primers used for  
29  
30 amplification of mouse RelA, c-mip and RNA18S transcripts, as well as quantitative PCR  
31  
32 conditions are listed in Table 2.  
33  
34  
35

36  
37 The wild-type and RelA-deficient mouse embryonic fibroblasts (MEF) were a kind gift of  
38  
39 Ron Hay (University of Dundee, Dundee, UK). RelA<sup>-/-</sup> MEF cells were derived from the  
40  
41 original RelA knockout mice and have been described previously.<sup>41</sup> MEF cells were  
42  
43 synchronized in DMEM containing 2% FCS, then cultured in DMEM containing 10% FCS,  
44  
45 in which Sorafenib was added at a concentration of 10  $\mu\text{M}$  for 24 hours.  
46  
47  
48  
49

### 50 51 ***Isolation of c-mip promoter, plasmid constructs and dual-luciferase reporter assays***

52  
53 We used 5'-RACE (rapid amplification of cDNA ends) to isolate the 5'UTR (untranslated  
54  
55 region) of c-mip using the primers indicated in Table 2. We selected oligonucleotides  
56  
57 spanning the 5' sequence of c-mip and the genomic DNA sequence upstream of the 5'UTR to  
58  
59  
60

1  
2  
3 amplify a 1270 bp DNA fragment by PCR from human genomic DNA. The PCR product was  
4  
5 verified by sequencing.  
6

7 The human c-mip-luciferase reporter plasmid (pGl<sub>3</sub>-C-mip-luc) was constructed by ligation of  
8  
9 a 1244 bp DNA fragment containing the c-mip promoter including the transcriptional start  
10  
11 site, into pGl<sub>3</sub>-Basic (Promega) predigested with NcoI/SmaI. All constructions were verified  
12  
13 by sequencing. The NF-κB p65/RelA and p50 expression plasmids have been described  
14  
15 elsewhere.<sup>42</sup> Dual-luciferase reporter assays driven by the c-mip promoter were performed as  
16  
17 previously reported.<sup>43</sup>  
18  
19

### 20 21 22 23 ***Chromatin immunoprecipitation (ChIP) and electrophoretic mobility shift assays (EMSA)***

24 To determine whether RelA binds *in vivo* to a specific sequence of the c-mip promoter, we  
25  
26 performed chromatin immunoprecipitation in a podocyte cell line, using the protocol  
27  
28 developed by Farnham PJ,<sup>44</sup> with minor modifications. Chromatin was sonicated on ice using  
29  
30 six pulses of 15 sec each at amplitude 3 on a Gene Pulser (Vibra Cell model 75022). A rabbit  
31  
32 polyclonal anti-RelA antibody (Santa Cruz Biotechnology) and rabbit IgG (control) were used  
33  
34 to immunoprecipitate RelA-containing chromatin. The immunoprecipitated chromatin was  
35  
36 treated with proteinase K, purified with a PCR cleanup kit (Qiagen), and concentrated by  
37  
38 precipitation with 0.3M NaCl. The PCR primers and conditions used to amplify the murine c-  
39  
40 mip proximal promoter and the sequences flanking the putative RelA site  
41  
42 (CAGGGGCTGCCCC) are indicated in Table 2.  
43  
44  
45

46 The preparation of nuclear fractions and EMSA experiments were performed as previously  
47  
48 described.<sup>45</sup>  
49  
50

### 51 52 53 ***Western blot analyses and immunoprecipitations***

54 The primary antibodies used in this study included anti- IκBα (rabbit and mouse),  
55  
56 anti-phospho-Ser<sup>32/36</sup> IκBα (ref 9242, 4814 and 9246, respectively, from Upstate Cell  
57  
58  
59  
60

1  
2  
3 signaling, USA), anti-RelA and anti-phospho-Ser<sup>276</sup> IκBα (sc-109 and sc-101749,  
4  
5 respectively, from Santa Cruz Biotechnology, Inc, USA), anti-Sp1 (Poly6247, BioLegend,  
6  
7 CA), anti-Calpain (ref 208737, Calbiochem, Germany). The c-mip polyclonal antibody was  
8  
9 produced in rabbits immunized with peptides raised against peptides located in PH and LRR  
10  
11 domains.  
12

13  
14 Cell protein extracts from podocyte or MEF cells were prepared in lysis buffer B (150 mM  
15  
16 NaCl, 10 mM Tris HCl pH 7.5, 2 mM DTT, 10% glycerol, 1 mM EDTA, 1% NP40, 1 mM  
17  
18 protease inhibitors, 1 mM NaF, and 1 mM sodium orthovanadate).  
19

20  
21 Cytosolic and nuclear fractions were prepared essentially as described previously.<sup>46</sup> Protein  
22  
23 concentrations were assayed using the Bio-Rad dye reagent (Bio-Rad, Richmond, CA),  
24  
25 following the instructions provided by the manufacturer. Immunoprecipitation experiments  
26  
27 were performed as previously described.<sup>34</sup>  
28  
29  
30  
31

### 32 **Statistical Analysis**

33  
34 Data represent the mean ± SEM and were prepared using GraphPad Prism software, version  
35  
36 4.0. We used the Mann-Whitney test or one-way Anova to evaluate P values.  
37  
38  
39  
40  
41  
42  
43  
44  
45  
46  
47  
48  
49  
50  
51  
52  
53  
54  
55  
56  
57  
58  
59  
60



1  
2  
3  
4  
5  
6  
7  
8  
9  
10  
11  
12  
13  
14  
15  
16  
17  
18  
19  
20  
21  
22  
23  
24  
25  
26  
27  
28  
29  
30  
31  
32  
33  
34  
35  
36  
37  
38  
39  
40  
41  
42  
43  
44  
45  
46  
47  
48  
49  
50  
51  
52  
53  
54  
55  
56  
57  
58  
59  
60

**Disclosure**

All the authors declared no competing interests.

For Peer Review Only

## References

1. Muller-Deile J, Worthmann K, Saleem M, *et al.* The balance of autocrine VEGF-A and VEGF-C determines podocyte survival. *Am J Physiol Renal Physiol* 2009; **297**: F1656-1667.
2. Guan F, Villegas G, Teichman J, *et al.* Autocrine VEGF-A system in podocytes regulates podocin and its interaction with CD2AP. *Am J Physiol Renal Physiol* 2006; **291**: F422-428.
3. Ivy SP, Wick JY, Kaufman BM. An overview of small-molecule inhibitors of VEGFR signaling. *Nat Rev Clin Oncol* 2009; **6**: 569-579.
4. Kerbel RS. Tumor angiogenesis. *N Engl J Med* 2008; **358**: 2039-2049.
5. Maharaj AS, Saint-Geniez M, Maldonado AE, *et al.* Vascular endothelial growth factor localization in the adult. *Am J Pathol* 2006; **168**: 639-648.
6. Neufeld G, Cohen T, Gengrinovitch S, *et al.* Vascular endothelial growth factor (VEGF) and its receptors. *FASEB J* 1999; **13**: 9-22.
7. Shweiki D, Itin A, Soffer D, *et al.* Vascular endothelial growth factor induced by hypoxia may mediate hypoxia-initiated angiogenesis. *Nature* 1992; **359**: 843-845.
8. Heinrich MC, Corless CL, Duensing A, *et al.* PDGFRA activating mutations in gastrointestinal stromal tumors. *Science* 2003; **299**: 708-710.

- 1  
2  
3  
4  
5 9. Hurwitz H, Fehrenbacher L, Novotny W, *et al.* Bevacizumab plus irinotecan,  
6 fluorouracil, and leucovorin for metastatic colorectal cancer. *N Engl J Med* 2004; **350**:  
7 2335-2342.  
8  
9  
10
- 11  
12  
13  
14 10. Waller CF. Imatinib mesylate. *Recent Results Cancer Res* 2010; **184**: 3-20.  
15  
16  
17
- 18  
19 11. Homsy J, Daud AI. Spectrum of activity and mechanism of action of VEGF/PDGF  
20 inhibitors. *Cancer Control* 2007; **14**: 285-294.  
21  
22  
23
- 24  
25 12. Eremina V, Jefferson JA, Kowalewska J, *et al.* VEGF inhibition and renal thrombotic  
26 microangiopathy. *N Engl J Med* 2008; **358**: 1129-1136.  
27  
28  
29
- 30  
31 13. Mathieson PW. Minimal change nephropathy and focal segmental glomerulosclerosis.  
32 *Semin Immunopathol* 2007; **29**: 415-426.  
33  
34  
35
- 36  
37 14. Sanz AB, Sanchez-Nino MD, Ramos AM, *et al.* NF-kappaB in renal inflammation. *J*  
38 *Am Soc Nephrol* 2010; **21**: 1254-1262.  
39  
40  
41  
42  
43  
44
- 45 15. Nowak DE, Tian B, Jamaluddin M, *et al.* RelA Ser276 phosphorylation is required for  
46 activation of a subset of NF-kappaB-dependent genes by recruiting cyclin-dependent  
47 kinase 9/cyclin T1 complexes. *Mol Cell Biol* 2008; **28**: 3623-3638.  
48  
49  
50  
51  
52  
53  
54  
55  
56  
57  
58  
59  
60

- 1  
2  
3 16. Zhong H, Voll RE, Ghosh S. Phosphorylation of NF-kappa B p65 by PKA stimulates  
4 transcriptional activity by promoting a novel bivalent interaction with the coactivator  
5 CBP/p300. *Mol Cell* 1998; **1**: 661-671.  
6  
7  
8  
9
- 10  
11  
12 17. Arun P, Brown MS, Ehsanian R, *et al.* Nuclear NF-kappaB p65 phosphorylation at  
13 serine 276 by protein kinase A contributes to the malignant phenotype of head and  
14 neck cancer. *Clin Cancer Res* 2009; **15**: 5974-5984.  
15  
16  
17  
18  
19
- 20  
21 18. Izzedine H, Massard C, Spano JP, *et al.* VEGF signalling inhibition-induced  
22 proteinuria: Mechanisms, significance and management. *Eur J Cancer* 2010; **46**: 439-  
23 448.  
24  
25  
26  
27  
28
- 29  
30 19. Roncone D, Satoskar A, Nadasdy T, *et al.* Proteinuria in a patient receiving anti-  
31 VEGF therapy for metastatic renal cell carcinoma. *Nat Clin Pract Nephrol* 2007; **3**:  
32 287-293.  
33  
34  
35  
36  
37
- 38  
39 20. Frangie C, Lefaucheur C, Medioni J, *et al.* Renal thrombotic microangiopathy caused  
40 by anti-VEGF-antibody treatment for metastatic renal-cell carcinoma. *Lancet Oncol*  
41 2007; **8**: 177-178.  
42  
43  
44  
45
- 46  
47 21. Izzedine H, Brocheriou I, Deray G, *et al.* Thrombotic microangiopathy and anti-VEGF  
48 agents. *Nephrol Dial Transplant* 2007; **22**: 1481-1482.  
49  
50  
51  
52
- 53  
54 22. Bollee G, Patey N, Cazajous G, *et al.* Thrombotic microangiopathy secondary to  
55 VEGF pathway inhibition by sunitinib. *Nephrol Dial Transplant* 2009; **24**: 682-685.  
56  
57  
58  
59  
60

- 1  
2  
3  
4  
5 23. Henke N, Schmidt-Ullrich R, Dechend R, *et al.* Vascular endothelial cell-specific NF-  
6 kappaB suppression attenuates hypertension-induced renal damage. *Circ Res* 2007;  
7  
8 **101**: 268-276.  
9  
10  
11  
12  
13  
14 24. Guzik TJ, Harrison DG. Endothelial NF-kappaB as a mediator of kidney damage: the  
15 missing link between systemic vascular and renal disease? *Circ Res* 2007; **101**: 227-  
16  
17 229.  
18  
19  
20  
21  
22  
23 25. Takase O, Marumo T, Imai N, *et al.* NF-kappaB-dependent increase in intrarenal  
24 angiotensin II induced by proteinuria. *Kidney Int* 2005; **68**: 464-473.  
25  
26  
27  
28  
29  
30 26. Yang JC, Haworth L, Sherry RM, *et al.* A randomized trial of bevacizumab, an anti-  
31 vascular endothelial growth factor antibody, for metastatic renal cancer. *N Engl J Med*  
32  
33 2003; **349**: 427-434.  
34  
35  
36  
37  
38  
39 27. Thakker GD, Hajjar DP, Muller WA, *et al.* The role of phosphatidylinositol 3-kinase  
40 in vascular endothelial growth factor signaling. *J Biol Chem* 1999; **274**: 10002-10007.  
41  
42  
43  
44  
45 28. Lamalice L, Houle F, Huot J. Phosphorylation of Tyr1214 within VEGFR-2 triggers  
46 the recruitment of Nck and activation of Fyn leading to SAPK2/p38 activation and  
47  
48 endothelial cell migration in response to VEGF. *J Biol Chem* 2006; **281**: 34009-34020.  
49  
50  
51  
52  
53  
54  
55  
56  
57  
58  
59  
60

- 1  
2  
3  
4  
5  
6  
7  
8  
9  
10  
11  
12  
13  
14  
15  
16  
17  
18  
19  
20  
21  
22  
23  
24  
25  
26  
27  
28  
29  
30  
31  
32  
33  
34  
35  
36  
37  
38  
39  
40  
41  
42  
43  
44  
45  
46  
47  
48  
49  
50  
51  
52  
53  
54  
55  
56  
57  
58  
59  
60
29. Gong C, Stoletov KV, Terman BI. VEGF treatment induces signaling pathways that regulate both actin polymerization and depolymerization. *Angiogenesis* 2004; **7**: 313-321.
  30. Veron D, Reidy KJ, Bertuccio C, *et al.* Overexpression of VEGF-A in podocytes of adult mice causes glomerular disease. *Kidney Int* 2010; **77**: 989-999.
  31. Bertuccio C, Veron D, Aggarwal PK, *et al.* Vascular Endothelial Growth Factor Receptor 2 Direct Interaction with Nephrin Links VEGF-A Signals to Actin in Kidney Podocytes. *J Biol Chem* 2011; **286**: 39933-39944.
  32. Sison K, Eremina V, Baelde H, *et al.* Glomerular structure and function require paracrine, not autocrine, VEGF-VEGFR-2 signaling. *J Am Soc Nephrol* 2010; **21**: 1691-1701.
  33. Echeverria V, Burgess S, Gamble-George J, *et al.* Sorafenib inhibits nuclear factor kappa B, decreases inducible nitric oxide synthase and cyclooxygenase-2 expression, and restores working memory in APPswe mice. *Neuroscience* 2009; **162**: 1220-1231.
  34. Zhang SY, Kamal M, Dahan K, *et al.* c-mip impairs podocyte proximal signaling and induces heavy proteinuria. *Sci Signal* 2010; **3**: ra39.
  35. Fremeaux-Bacchi V, Moulton EA, Kavanagh D, *et al.* Genetic and functional analyses of membrane cofactor protein (CD46) mutations in atypical hemolytic uremic syndrome. *J Am Soc Nephrol* 2006; **17**: 2017-2025.

- 1  
2  
3  
4  
5 36. Veyradier A, Obert B, Houllier A, *et al.* Specific von Willebrand factor-cleaving  
6 protease in thrombotic microangiopathies: a study of 111 cases. *Blood* 2001; **98**:  
7 1765-1772.  
8  
9  
10  
11  
12  
13  
14 37. Tesch GH, Hill PA, Wei M, *et al.* LF15-0195 prevents the induction and inhibits the  
15 progression of rat anti-GBM disease. *Kidney Int* 2001; **60**: 1354-1365.  
16  
17  
18  
19  
20  
21 38. Rangan GK, Tesch GH. Quantification of renal pathology by image analysis.  
22 *Nephrology (Carlton)* 2007; **12**: 553-558.  
23  
24  
25  
26  
27 39. Tokuyasu KT. A technique for ultracryotomy of cell suspensions and tissues. *J Cell*  
28 *Biol* 1973; **57**: 551-565.  
29  
30  
31  
32  
33  
34 40. Mundel P, Reiser J, Zuniga Mejia Borja A, *et al.* Rearrangements of the cytoskeleton  
35 and cell contacts induce process formation during differentiation of conditionally  
36 immortalized mouse podocyte cell lines. *Exp Cell Res* 1997; **236**: 248-258.  
37  
38  
39  
40  
41  
42  
43 41. Beg AA, Sha WC, Bronson RT, *et al.* Embryonic lethality and liver degeneration in  
44 mice lacking the RelA component of NF-kappa B. *Nature* 1995; **376**: 167-170.  
45  
46  
47  
48  
49 42. Thanos D, Maniatis T. The high mobility group protein HMG I(Y) is required for NF-  
50 kappa B- dependent virus induction of the human IFN-beta gene. *Cell* 1992; **71**: 777-  
51 789.  
52  
53  
54  
55  
56  
57  
58  
59  
60

- 1  
2  
3  
4  
5  
6  
7  
8  
9  
10  
11  
12  
13  
14  
15  
16  
17  
18  
19  
20  
21  
22  
23  
24  
25  
26  
27  
28  
29  
30  
31  
32  
33  
34  
35  
36  
37  
38  
39  
40  
41  
42  
43  
44  
45  
46  
47  
48  
49  
50  
51  
52  
53  
54  
55  
56  
57  
58  
59  
60
43. Kamal M, Valanciute A, Dahan K, *et al.* C-mip interacts physically with RelA and inhibits nuclear factor kappa B activity. *Mol Immunol* 2009; **46**: 991-998.
44. Wells J, Farnham PJ. Characterizing transcription factor binding sites using formaldehyde crosslinking and immunoprecipitation. *Methods* 2002; **26**: 48-56.
45. Sahali D, Pawlak A, Le Gouvello S, *et al.* Transcriptional and post-transcriptional alterations of IkappaBalpha in active minimal-change nephrotic syndrome. *J Am Soc Nephrol* 2001; **12**: 1648-1658.
46. Stein B, Rahmsdorf HJ, Steffen A, *et al.* UV-induced DNA damage is an intermediate step in UV-induced expression of human immunodeficiency virus type 1, collagenase, c-fos, and metallothionein. *Mol Cell Biol* 1989; **9**: 5169-5181.



## Legends

### **Figure 1. Differential expression of VEGF, HIF1 $\alpha$ , c-mip, RelA and Tie2 in glomeruli of patients with MCN/FSG-like lesions or TMA following anti-VEGF or RTKI therapies.**

Representative immunohistochemical analysis of VEGF (a), c-mip (b), HIF1 $\alpha$  (c), RelA (d) and Tie-2 (e) in kidney biopsies of patients with renal diseases associated with anti-VEGF drugs. Note that VEGF is not detected in TMA, whereas it is little reduced in MCN-FSG-like lesions. C-mip is not detected in the glomeruli of control human kidneys (Con) or in thrombotic microangiopathy (TMA), while it is clearly visualized along the external side of the glomerular capillary loops in minimal change nephropathy (MCN). The expression of HIF-1 $\alpha$  is highly increased in TMA glomeruli, while it is scarcely detectable in MCN/FSG-like lesions. Within TMA glomeruli, HIF-1 $\alpha$  is mostly restricted to podocyte nuclei. The abundance of RelA is strongly increased in segmental pattern in TMA glomeruli, whereas it is decreased in MCN/FSG-like lesions, as compared to control glomeruli (Con). Tie2 was significantly upregulated after anti-VEGF or RTKI therapies. Scale bars, 20  $\mu$ m. The relative abundance of these markers was measured by computer-assisted image analysis using 400x magnification and shown in (f). MCN/FSG-RTKI: Minimal Change nephropathy/focal and segmental glomerulosclerosis induced by RTKI. idiopathic MCNS. iFSG: idiopathic FSGS. TMAveg: TMA induced by VEGF. iTMA: idiopathic TMA

### **Figure 2. Differential expression of RelA and nephrin in TMA and MCN-like lesions.**

Confocal microscopy analysis of nephrin (red) and RelA (green) expression in control human kidneys (Con), MCN-like lesions (MCN) and TMA biopsies. The abundance of RelA is significantly increased in TMA. RelA is colocalized with nephrin but it is also abundant inside of the capillary loops, within the TMA glomeruli. Scale bars, 10  $\mu$ m.

1  
2  
3  
4  
5 **Figure 3. Differential expression of RelA and Tie2 in TMA and MCN-like lesions.**

6  
7 Confocal microscopy analysis of Tie2 (red) and RelA (green) expression in control glomeruli  
8 (Con), MCN-like lesions (MCN) and TMA biopsies. The abundance of RelA and Tie2 is  
9 significantly increased in TMA. Tie2 and RelA are colocalized in damaged areas within TMA  
10 glomeruli, whereas they are expressed in different cell compartments in control glomeruli.  
11  
12 Scale bars, 10  $\mu\text{m}$ .  
13  
14  
15  
16  
17  
18  
19

20  
21 **Figure 4. Overproduction of RelA in endothelial cells in TMA.** Confocal microscopy

22 analysis of Tie2 (red) and RelA (green) expression in arterioles of control human kidneys  
23 (Con), and TMA biopsies. The abundance of RelA and Tie2 is significantly increased in TMA  
24 arterioles, which display a swelling of endothelial cells. The abundance of RelA is also  
25 increased in the pericytes of TMA arterioles. Scale bars, 10  $\mu\text{m}$ . The relative abundance of  
26 RelA was assessed by quantifying the specific arteriolar fluorescence intensity in 3-D stacks  
27 of images taken by confocal microscopy and normalized to total arteriolar area. Five samples  
28 were analyzed in each condition (Con and TMA). Data represent the mean  $\pm$  sem (\* $P < 0.05$ ,  
29 Mann Whitney test).  
30  
31  
32  
33  
34  
35  
36  
37  
38  
39  
40  
41  
42

43 **Figure 5. Electron microscopy analysis and distribution of RelA by immunogold labeling**

44 **in TMA. (a)** Representative transmission electron micrographs of the glomeruli in a patient  
45 with bevacizumab-induced TMA (right panel) and in a control kidney (left panel). **(b)**  
46 Representative immunogold labelling for Rel A (10 nm gold, indicated by the asterisks) in the  
47 glomeruli of a patient with bevacizumab-induced TMA (right panel) and in a control kidney  
48 (left panel). **(c)** Quantification of gold label for RelA in glomeruli patients with TMA (n=3)  
49  
50  
51  
52  
53  
54  
55  
56  
57  
58  
59  
60

1  
2  
3 and in control (n=3) (NS, non significant, P=0.6993; \*\*P=0.0026; \*\*\*P=0.0006, Mann  
4  
5 Whitney test).  
6  
7  
8

9  
10 **Figure 6. RelA binds to c-mip promoter and prevents its transcriptional activity. (a)**

11 characterization of the c-mip promoter. Nucleotide sequence of the human c-mip proximal  
12 promoter region. Nucleotides are numbered to the left of the sequence with the transcription  
13 start site (TSS) indicated by the position +1. The potential CCAAT site and NF- $\kappa$ B  
14 responsive element (NF- $\kappa$ B RE) are indicated. **(b)** identification of NF- $\kappa$ B RE by chromatin  
15 immunoprecipitation. HEK cells were cross-linked with formaldehyde, and chromatin was  
16 immunoprecipitated with antibodies against rabbit polyclonal anti-RelA antibody or rabbit  
17 IgG (control). Immunoprecipitated DNA was analyzed by PCR using primers flanking the  
18 NF- $\kappa$ B RE within the human promoter (the region amplified spans from -279 to -72 relative  
19 to the transcriptional start site). **(c)** RelA binds to NF- $\kappa$ B recognition site on the c-mip  
20 promoter. HEK cells were transiently co-transfected with either RelA expression plasmid or  
21 its empty vector (Ev). Protein extracts (20  $\mu$ g) were used for NF- $\kappa$ B DNA-binding assays.  
22 Nuclear extracts were incubated with the wild-type NF- $\kappa$ B oligonucleotide in the absence or  
23 presence of anti-RelA/p65 antibody. The specificity of NF- $\kappa$ B interaction was monitored by  
24 using a mutant NF- $\kappa$ B oligonucleotide. The quantification of NF- $\kappa$ B band shifts is indicated.  
25  
26  
27  
28  
29  
30  
31  
32  
33  
34  
35  
36  
37  
38  
39  
40  
41  
42  
43  
44 **(d)** RelA inhibits the c-mip promoter-dependent luciferase activity. HEK cells were co-  
45 transfected with the NF- $\kappa$ B (RelA/p65, p50) expression plasmids and the human c-mip  
46 luciferase reporter plasmid (pGL<sub>3</sub>-C-mip-luc). The phRL-null vector was used as an internal  
47 control for transfection. Cell extracts were prepared 24h after transfection, then luciferase  
48 activity was measured and normalized by protein content determined by using a Bradford  
49 assay. Data are presented as relative luciferase activity (firefly luciferase/the renilla  
50  
51  
52  
53  
54  
55  
56  
57  
58  
59  
60

1  
2  
3 luciferase). The two-tailed t-test is used for statistical analysis (\*\*\*)  $P < 0.001$ , Mann Whitney  
4 test). Five independent experiments were performed.  
5  
6  
7

8  
9  
10 **Figure 7. Overproduction of c-mip in RelA-deficient cells.** Relative expression of *RelA* and  
11 *c-mip* transcripts on total RNA from wild-type and RelA-deficient MEF. Bars represent mean  
12 value of five independent experiments with error bars indicating SEM (\*\*\*)  $P < 0.001$ , Mann  
13 Whitney test).  
14  
15  
16  
17

18  
19  
20  
21 **Figure 8. RTKI sorafenib induces an upregulation of c-mip.** (a) Left, Western-blot  
22 analysis of c-mip on total protein lysates from wild-type and RelA-deficient MEF, with or  
23 without treatment by sorafenib (10  $\mu\text{M}$ ). The membrane was reblotted with GAPDH  
24 antibody; left, relative abundance of c-mip corrected by GAPDH signal (from left panel).  
25 Similar results were obtained in two independent experiments. (b) Relative expression of *c-*  
26 *mip* transcript on total RNA from differentiated podocytes non-treated or treated with  
27 Sorafenib (10  $\mu\text{M}$ ). Bars represent mean value of three independent experiments with error  
28 bars indicating SEM (\* $P < 0.05$ , Mann Whitney test). (c) Western-blot analysis of c-mip on  
29 total protein lysates from normal lymphocytes with (+) or without (-) treatment by sorafenib  
30 (10  $\mu\text{M}$ ).  
31  
32  
33  
34  
35  
36  
37  
38  
39  
40  
41  
42  
43  
44

45  
46 **Figure 9. Sorafenib inhibits RelA activation.** (a) Western-blot analysis of pSer<sup>32/36</sup> I $\kappa$ B $\alpha$   
47 and pSer<sup>276</sup> RelA on total protein lysates from podocytes, with (+) or without (-) treatment by  
48 sorafenib (10  $\mu\text{M}$ ). The quantification of phosphorylated forms on total proteins is indicated  
49 in the lower panels. Bars represent mean value of three independent experiments with error  
50 bars indicated SEM (\* $P < 0.05$ , one-way Anova test). (b) Western-blot analysis of RelA on  
51 cytoplasm and nuclear podocyte extracts of which the purity was assessed by calpain and Spl  
52  
53  
54  
55  
56  
57  
58  
59  
60

1  
2  
3 blotting, respectively. Data are representative of three independent experiments. **(c)**  
4  
5 Immunoprecipitation of RelA (rabbit antibody) from podocyte protein lysates, followed by  
6  
7 sequential immunoblotting with mouse  $\text{I}\kappa\text{B}\alpha$  and RelA antibodies. **(d)** Confocal microscopy  
8  
9 analysis of MEF cells with or without treatment by sorafenib (10  $\mu\text{M}$ ) for 48 hours. Similar  
10  
11 results were obtained with podocyte cell line.  
12  
13  
14  
15  
16  
17  
18  
19  
20  
21  
22  
23  
24  
25  
26  
27  
28  
29  
30  
31  
32  
33  
34  
35  
36  
37  
38  
39  
40  
41  
42  
43  
44  
45  
46  
47  
48  
49  
50  
51  
52  
53  
54  
55  
56  
57  
58  
59  
60

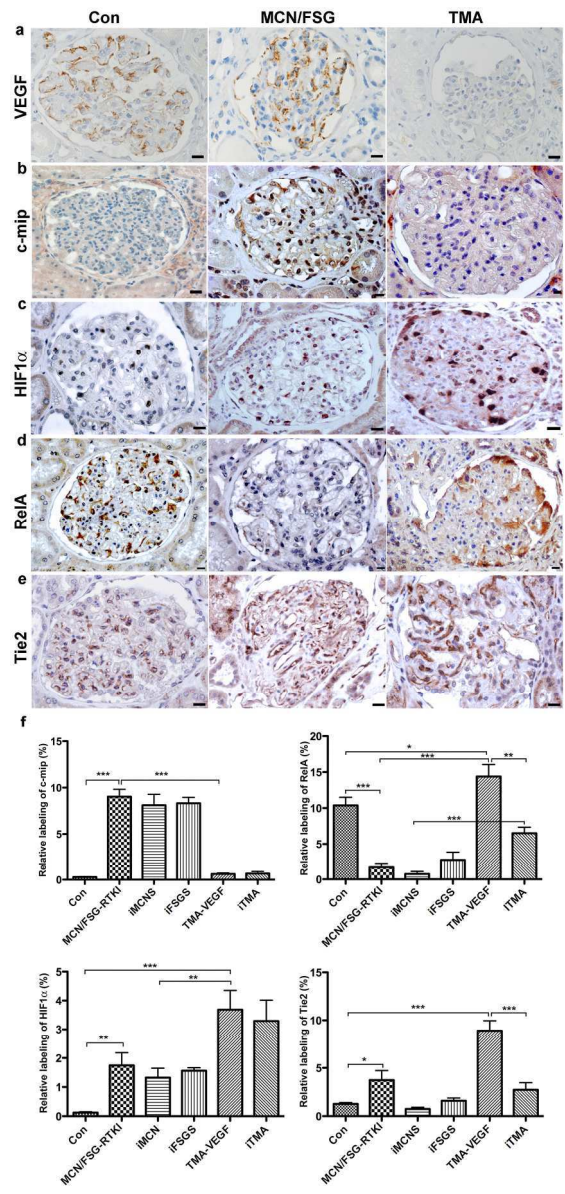
For Peer Review Only

### Acknowledgments

We would like to thank Pr Ronald T. Hay (University of Dundee, U.K.) for providing the wild type and RelA-deficient mouse embryonic fibroblasts (MEF), Pr Peter Mundel (Miller School of Medicine, University of Miami, USA) for providing the podocyte cell line, Dr Yves Allory (Pathology department) for providing us with renal samples.

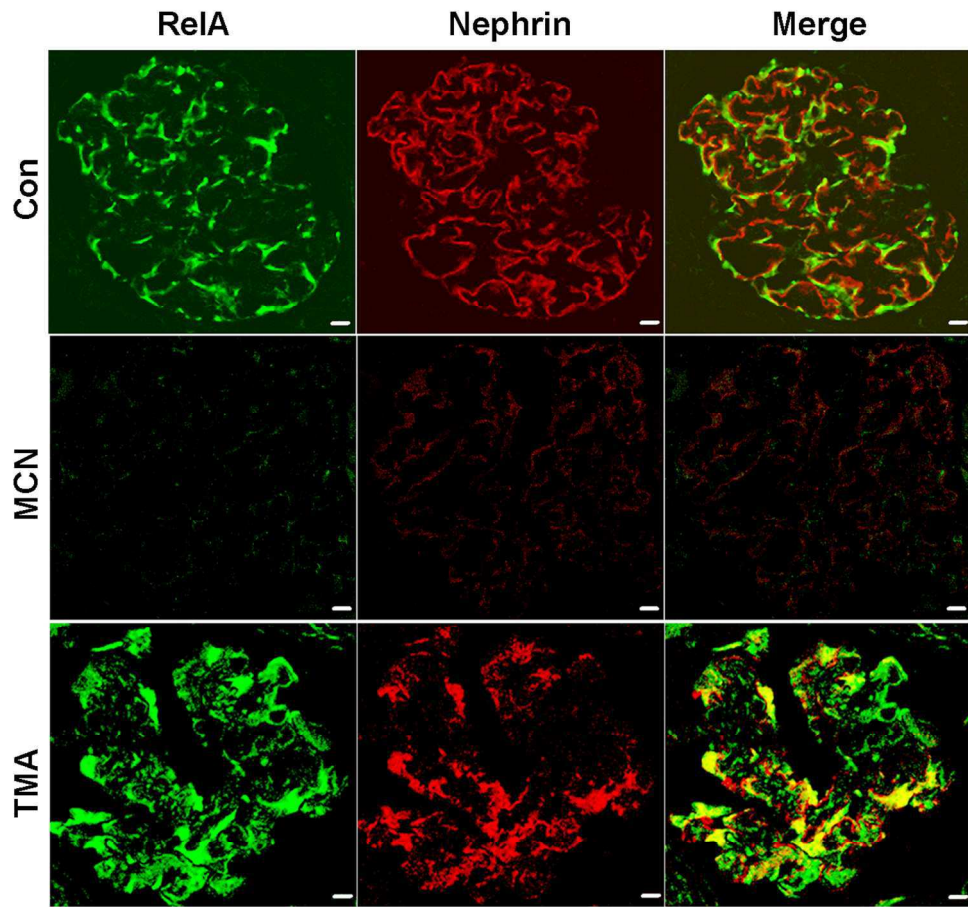
This work was supported in part by a grant from the French Kidney Foundation. M Mangier is supported by grants of Ministère de la Recherche V Ory was supported by grants of Ministère de la Recherche and from the French Society of Nephrology

1  
2  
3  
4  
5  
6  
7  
8  
9  
10  
11  
12  
13  
14  
15  
16  
17  
18  
19  
20  
21  
22  
23  
24  
25  
26  
27  
28  
29  
30  
31  
32  
33  
34  
35  
36  
37  
38  
39  
40  
41  
42  
43  
44  
45  
46  
47  
48  
49  
50  
51  
52  
53  
54  
55  
56  
57  
58  
59  
60



119x260mm (300 x 300 DPI)

1  
2  
3  
4  
5  
6  
7  
8  
9  
10  
11  
12  
13  
14  
15  
16  
17  
18  
19  
20  
21  
22  
23  
24  
25  
26  
27  
28  
29  
30  
31  
32  
33  
34  
35  
36  
37  
38  
39  
40  
41  
42  
43  
44  
45  
46  
47  
48  
49  
50  
51  
52  
53  
54  
55  
56  
57  
58  
59  
60



119x115mm (300 x 300 DPI)

Only



1  
2  
3  
4  
5  
6  
7  
8  
9  
10  
11  
12  
13  
14  
15  
16  
17  
18  
19  
20  
21  
22  
23  
24  
25  
26  
27  
28  
29  
30  
31  
32  
33  
34  
35  
36  
37  
38  
39  
40  
41  
42  
43  
44  
45  
46  
47  
48  
49  
50  
51  
52  
53  
54  
55  
56  
57  
58  
59  
60

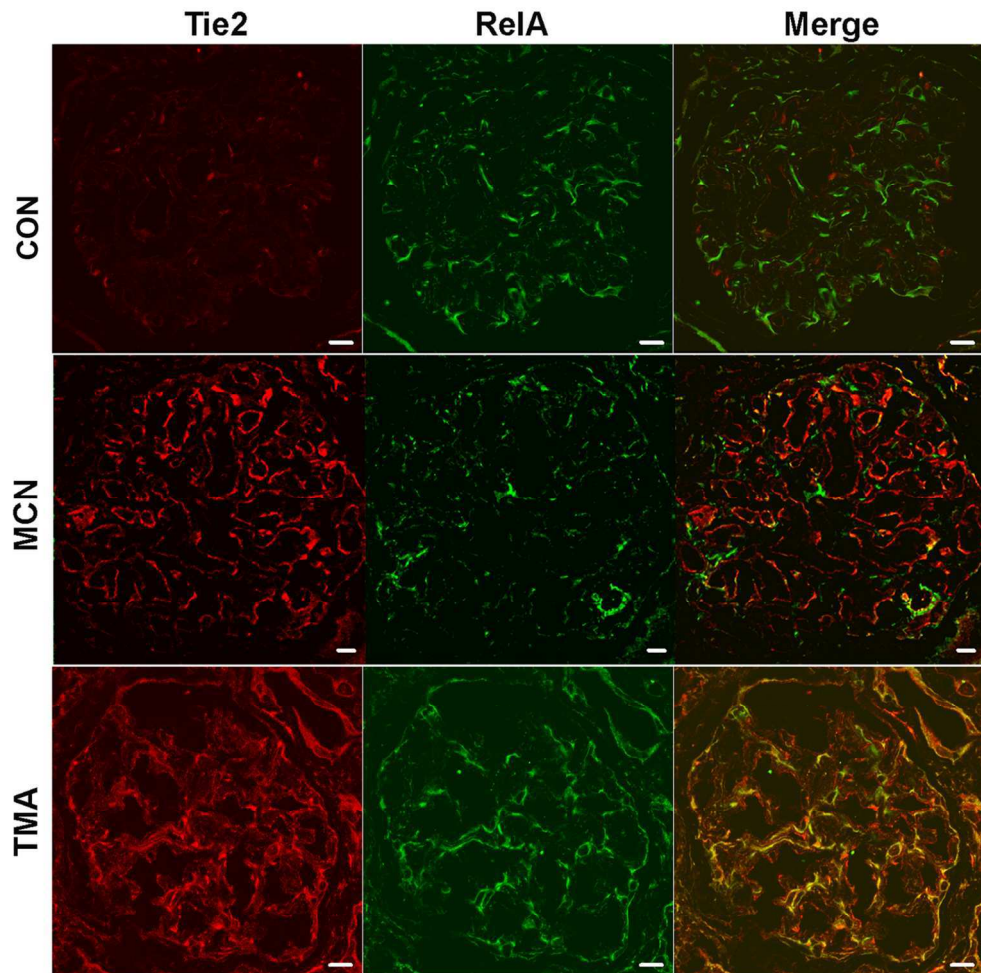
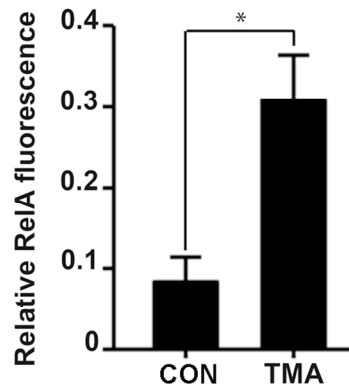
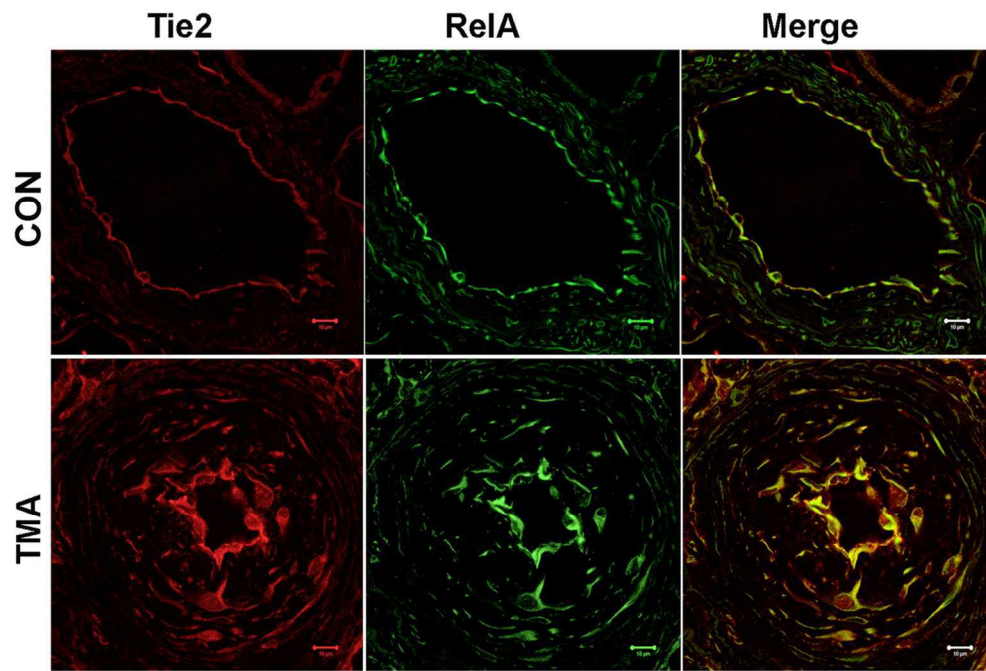


Fig. 3

119x124mm (300 x 300 DPI)



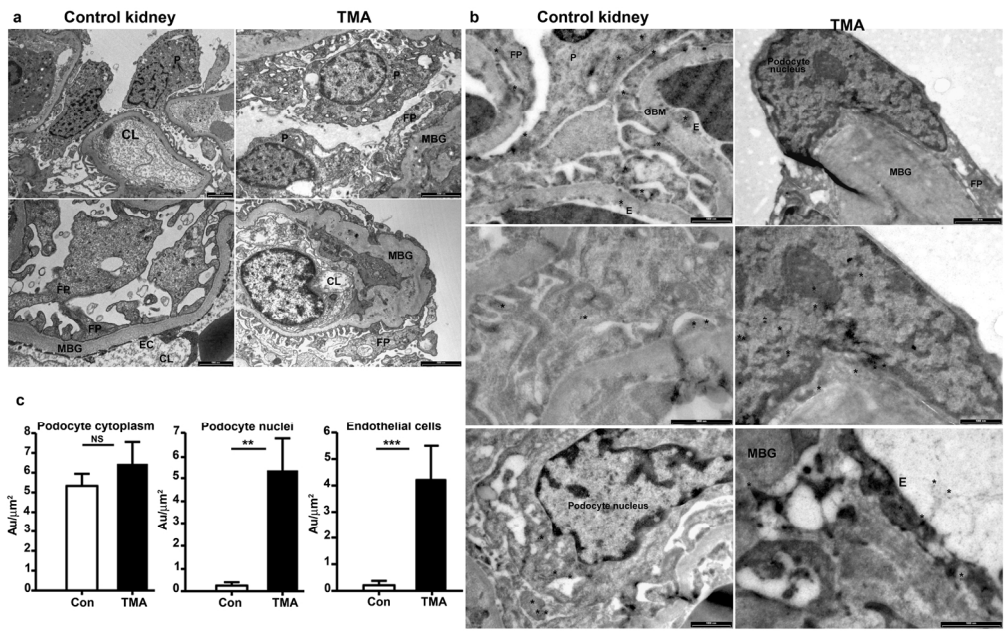


46  
47  
48  
49  
50  
51  
52  
53  
54  
55  
56  
57  
58  
59  
60

**Fig. 4**

119x137mm (300 x 300 DPI)

1  
2  
3  
4  
5  
6  
7  
8  
9  
10  
11  
12  
13  
14  
15  
16  
17  
18  
19  
20  
21  
22  
23  
24  
25  
26  
27  
28  
29  
30  
31  
32  
33  
34  
35  
36  
37  
38  
39  
40  
41  
42  
43  
44  
45  
46  
47  
48  
49  
50  
51  
52  
53  
54  
55  
56  
57  
58  
59  
60



160x99mm (300 x 300 DPI)

Review Only

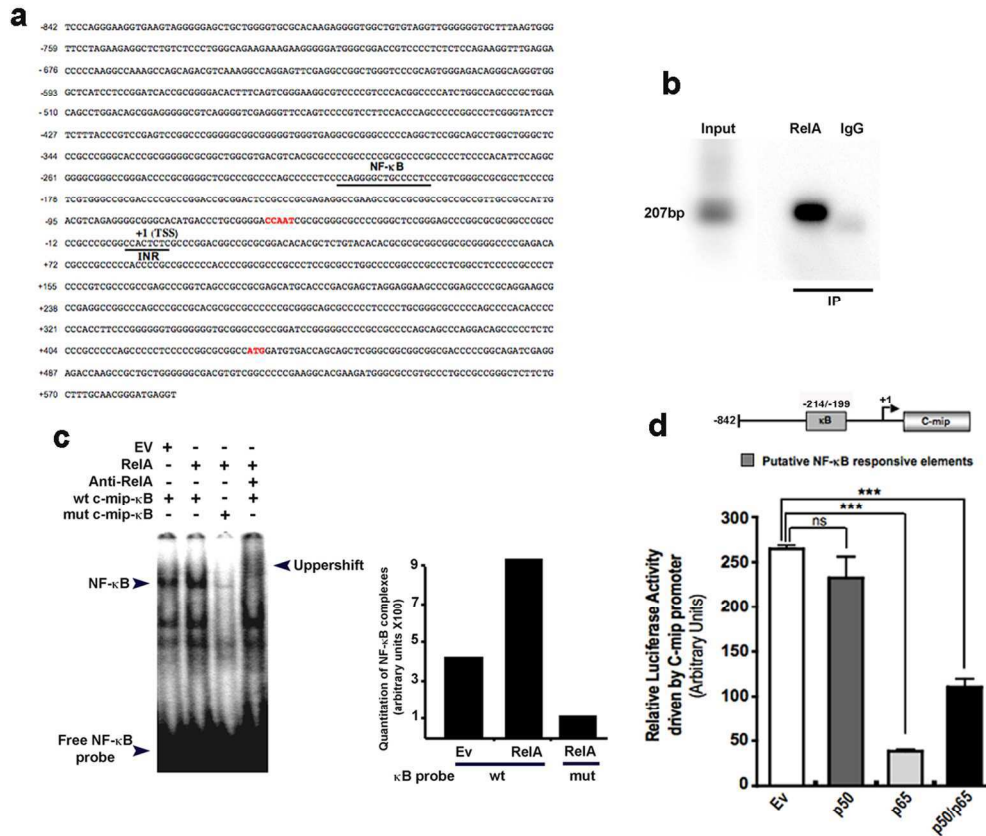


Fig. 6

119x109mm (300 x 300 DPI)

1  
2  
3  
4  
5  
6  
7  
8  
9  
10  
11  
12  
13  
14  
15  
16  
17  
18  
19  
20  
21  
22  
23  
24  
25  
26  
27  
28  
29  
30  
31  
32  
33  
34  
35  
36  
37  
38  
39  
40  
41  
42  
43  
44  
45  
46  
47  
48  
49  
50  
51  
52  
53  
54  
55  
56  
57  
58  
59  
60

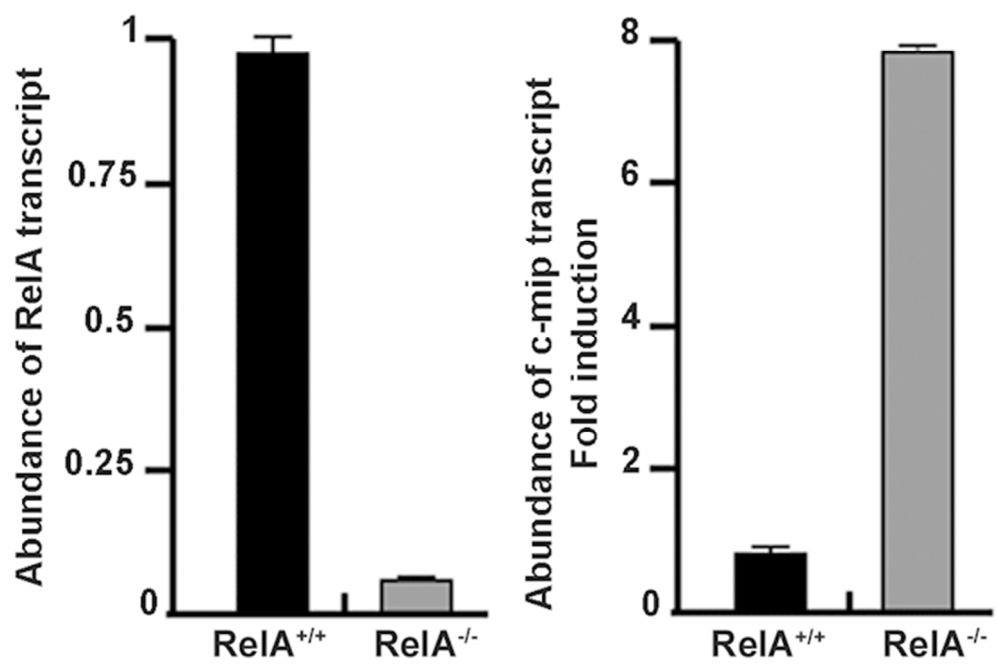


Fig. 7

60x45mm (300 x 300 DPI)

View Only

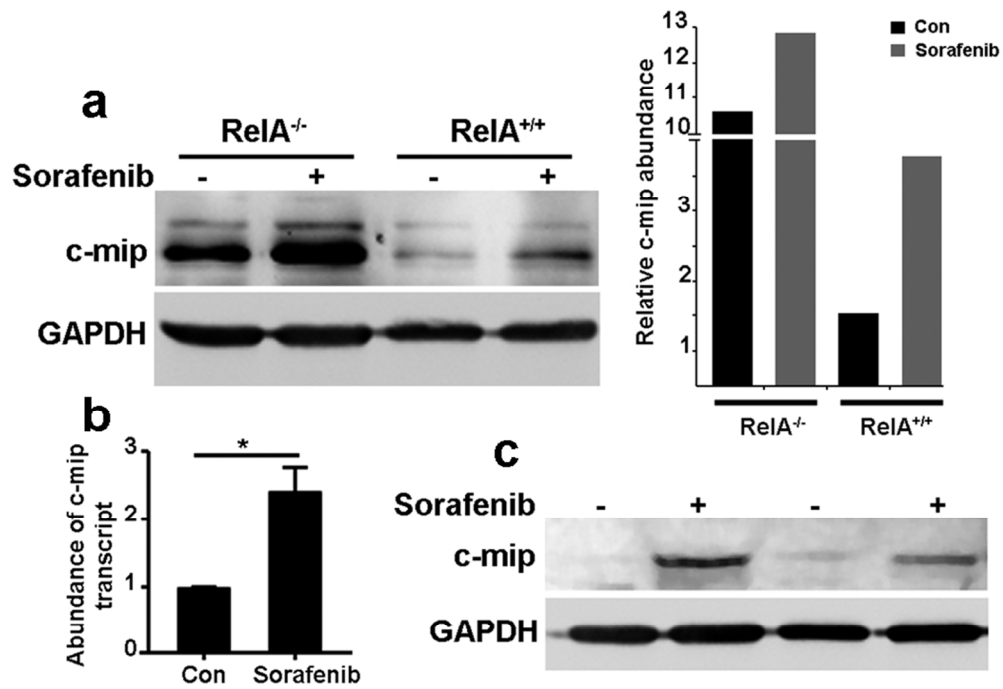
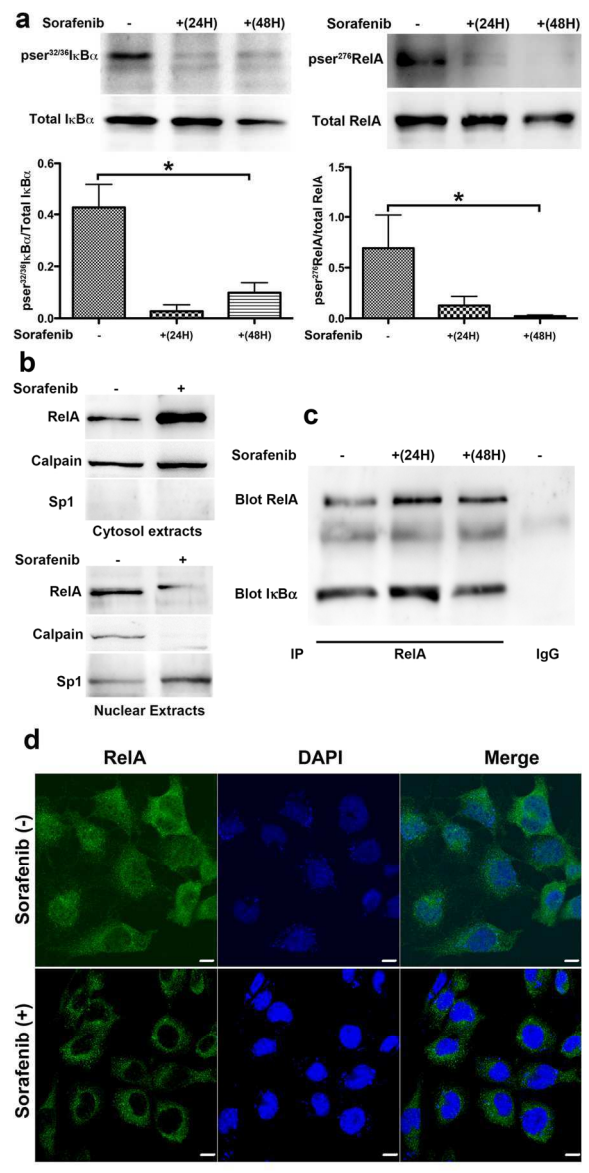


Fig. 8

86x64mm (300 x 300 DPI)

1  
2  
3  
4  
5  
6  
7  
8  
9  
10  
11  
12  
13  
14  
15  
16  
17  
18  
19  
20  
21  
22  
23  
24  
25  
26  
27  
28  
29  
30  
31  
32  
33  
34  
35  
36  
37  
38  
39  
40  
41  
42  
43  
44  
45  
46  
47  
48  
49  
50  
51  
52  
53  
54  
55  
56  
57  
58  
59  
60



86x180mm (300 x 300 DPI)

**Table 1: Patient characteristics at baseline**

	All patients	MCN/FSG	TMA
n	29	8	13
Men	19	6	3
Age, yr, mean (range)	55.2 (20-79)	71.5 (37-79)	69.5 (20-67)
mRCC	17	7	3
Previous nephrectomy	14	6	3
Previous radiotherapy and/or IFN $\alpha$ use	12	5	4
Anti-VEGF agents			
Bevacizumab (cumulative dose)	9	-	6 (10-240 mg/kg)
VEGF Trap (cumulative dose)	6	-	5 (12-54 mg/kg)
Sunitinib (cumulative dose)	11	5 (50-200 mg)	2 (100 mg)
Axitinib (cumulative dose)	1	1 (40 mg)	-
Sorafenib (cumulative dose)	3	2 (800 mg)	-
Renal parameters			
SBP, mmHg, mean (range)	150.0 (110-190)	130.0 (110-180)	165.0 (120-190)
DBP, mmHg, mean (range)	95.0 (60-115)	83.0 (60-110)	100.0 (80-115)
Proteinuria, g/day, mean (range)	3.50 (0.6-19.5)	3.5 (2-5,5)	4.11 (0.6-19.5)
Edema	14	5 (62.5%)	4 (31%)
Microhematuria	12	2 (28.5%)	6 (46%)
SCr, mg/dL, mean (range)	1.26 (0.70-4.44)	0.95 (0.79-1.27)	0.86 (0.70-1.45)
aMDRD CrCl, mL/min/1.73 m <sup>2</sup> , mean (range)	76.5 (13.7-120)	76 (17-102)	75 (45-120)
Outcome			
Follow up duration	1 mo – 3 yrs	3 yrs	6 mo – 2 yrs
Alive	14	1	8
SCr, mg/dL	1.0 (0.75-2.1)	1.20	0.95 (0.75-2.1)

MCN/FSG, minimal change nephropathy/focal segmental glomerulopathy, TMA, thrombotic microangiopathy; mRCC, metastatic renal cell carcinoma; IFN $\alpha$ , interferon alpha; VEGF, vascular endothelial growth factor; SBP, systolic blood pressure; DBP, diastolic blood pressure; SCr, serum creatinin; aMDRD CrCl, creatinine clearance; mo, month.



**Table 2. Sequence of primers and PCR conditions.**

Primers	Sequence	Accession number	Expected size	Ann Temp (°C)	PCR cycles
Mouse primers	c-mip Forward: CAGAGGTTTGCAGAAGATCCAAGA CAGGAA	XM924798	462	60	32
	Reverse: GCGGGCCAGGTCCGCATCC	NM_009045.4	420	60	30
	RelA Forward: GTGGAGATCATCGAACAGCCGAAG				
	Reverse: GCAGAGGCGCACTGCATTCAAGTC	NR_003278	151	60	16
	18S Forward: GTAACCCGTTGAACCCATT				
	Reverse: CCATCCAATCGGTAGTAGCG				
Mouse c-mip Proximal promoter	Forward CAGACATATACTACAAGTTGGCTTC GAACGCAC		1604	65	35
κB RE	Reverse CTAAGCTGTTGTCGGCCAGCGTTAGGTG				
EMSA	RE putative site: CAGGGGCTGCCCC				
Chip sequence	oligonucleotide (Forward strand): 5'CCAGGGGCTGCCCCCTC-3		207	58	35
	Forward: CCTCCCCACATTCCAGGCG Reverse: TCATGTGCCCCGCCCTCTG Internal probe: CGCGAGAGGCCGAAGCCGC				

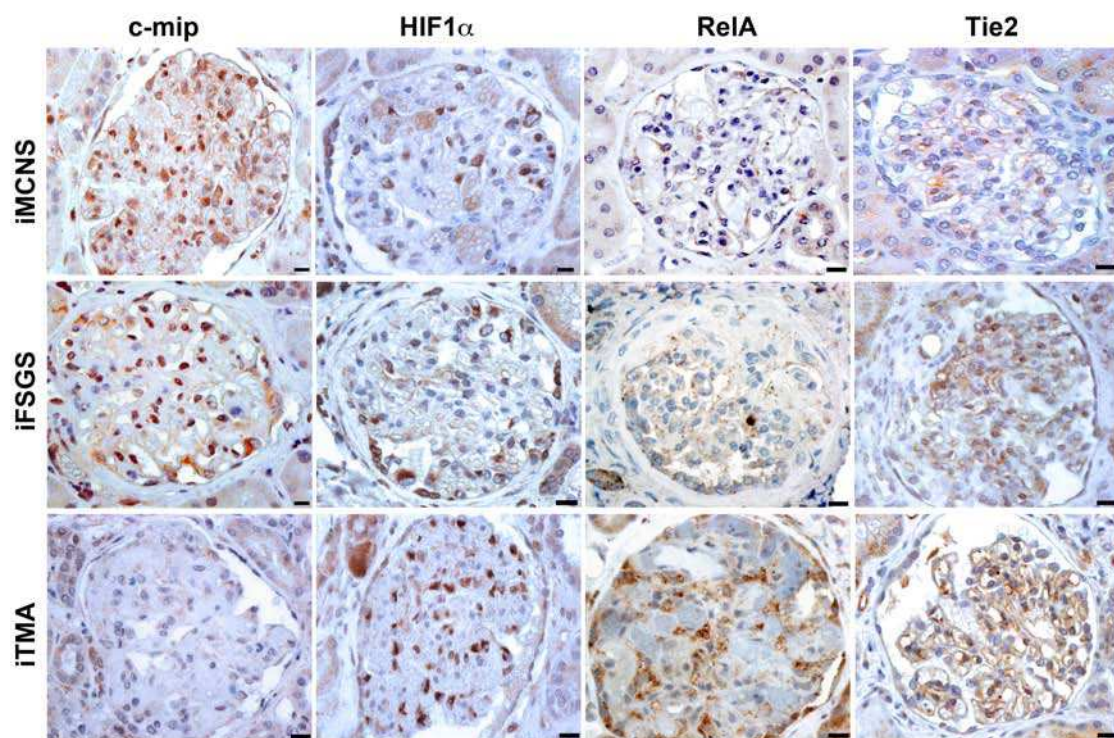


Figure S1: Representative immunohistochemical analysis of several markers in idiopathic glomerular diseases